The Egyptian Journal of Remote Sensing and Space Sciences 25 (2022) 473–489

HOSTED BY

Contents lists available at ScienceDirect

The Egyptian Journal of Remote Sensing and Space Sciences

journal homepage: www.sciencedirect.com

Detecting and mapping karst landforms using object-based image analysis: Case study: Takht-Soleiman and Parava Mountains, Iran ☆

Mohammad Kazemi Garajeh [a,*], Bakhtiar Feizizadeh [a,c], Thomas Blaschke [b], Tobia Lakes [c,d]

[a] Department of Remote Sensing and GIS, University of Tabriz, Tabriz, Iran
[b] Department of Geoinformatics Z_GIS, University of Salzburg, Salzburg, Austria
[c] Lab of Geoinformation Sciences, Department of Geography, Humboldt University of Berlin, Berlin, Germany
[d] IRI THESys, Humboldt-Universität zu Berlin, Germany

ARTICLE INFO

Article history:
Received 13 September 2021
Revised 26 February 2022
Accepted 15 March 2022
Available online 23 March 2022

Keywords:
Karst zones and landforms
Object-based image analysis
Spatial and spectral features
A semi-automated approach

ABSTRACT

This study presents a novel, semi-automated approach for integrating decision rules and object-based image analysis (OBIA) methods for identifying and mapping karst zones and landforms. We developed a multi-resolution segmentation approach using an Approximate Gaussian function to compute the degree of fuzzy memberships of object-based features and applied it to Sentinel-2 satellite images and a digital elevation model. The object based features and decision rules were applied to identify and detect karst landforms in the semi-automated approach. The efficiency of each technique was examined based on two case studies in Takht-Soleiman and Parava-Biston in Iran using a fuzzy synthetic evaluation (FSE) approach and ground control points. The validation of the karst landform detection and delineation yielded high accuracies for the six prominent landforms, namely Dolin (96.8%), Ouvala (99.2%), Lapiez (95.1%), Canyon (98.3%), Polje (96.1%) and Karren (97.4%), respectively. Based on the research outcome, we conclude that the combined use of spatial (e.g. shape index, compactness, asymmetry), spectral (e.g. brightness, mean and standard deviation) and textural (grey-level co-occurrence matrix, GLCM) features allows us to detect and map karst landforms efficiently. This fuzzy rule object-based approach can enhance the accuracy of geomorphological and geological maps and allows for a regular update of the usually labor-intensive geological mapping campaigns.

1. Introduction

Karst zones are the main source of drinking water in many regions (Kalhor et al., 2019). A karst area is a type of terrain that encompasses a significant thickness of limestone mass. Such limestone areas are characterized by interesting landforms that are created by underground drainage (Waltham and Fookes, 2005). Specifically, the karst landforms differentiated based on their features are the Dolin, Ouvala, Lapiez, Canyon, Aven, Polje, Karren and Cave. Maps showing the various landforms in a karst area are key in efficient water resource management because of the potential of these areas to store and transmit large quantities of water (Kalhor et al., 2019). Landforms exhibit the physiological and morphological characteristics of the earth, which can contribute to aid our understanding of past and presently active processes of it (Gerçek, 2010). Generally, landform information is available in analogue format in the form of geomorphological maps, which indicate land units based on their genesis, material and shape (Robson et al., 2020).

There are three approaches to exploring and recognizing karst phenomena, namely the engineering geological classification, drilling, and geophysical prospecting (Alexopoulos et al., 2011; Vargemezis et al., 2012; Zaidi and Kassem, 2012; Farooq et al., 2012; Putiska et al., 2014). However, these methods provide limited tools for identifying a karst area and mapping its landforms (Hofierka et al., 2018). The geophysical methods, for instance, provide some critical underground information such as a vulnerability evaluation and hazard calculation or groundwater exploration (Chalikakis et al., 2011). Mapping karst areas and the associated landforms still depends on traditional and manual mapping techniques (Groppelli and Viereck-Goette, 2010). Furthermore, the mapping of karst areas and their respective landforms is costly and labor-intensive due to the limited availability of data (Mohamed and Verstraeten, 2012). Hence, there is a significant

Peer review under responsibility of National Authority for Remote Sensing and Space Sciences.
* Corresponding author.
E-mail address: kazemi20.0432@gmail.com (M.K. Garajeh).

https://doi.org/10.1016/j.ejrs.2022.03.009
1110-9823/

need for faster methods that provide a low-cost option for identifying karst areas and mapping the associated landforms.

Satellite observation data now provides up-to-date spectral imagery with a high spatial and temporal resolution via different sensors with which we can detect the earth's landforms at the global scale (Pederson, 2016; Kazemi Garajeh and Feizizadeh, 2021). In this context, the benefits of using remote sensing imagery have led to the development of semi-automated and automated approaches for extracting and mapping environmental features based on their object-based properties, for example using object-based image analysis (OBIA) (Najafi et al., 2019; Kazemi Garajeh et al., 2021). Semi-automated OBIA uses object-based rule sets and applies them to a variety of satellite images. In the domain of remote sensing, this approach has gained prominence because of its ability to overcome the weaknesses of the traditional image processing techniques (e.g., the pixel-based approach) by integrating contextual and geometric information with the spectral properties (Drăguţ and Eisank, 2012; Feizizadeh et al., 2017). This rule-based approach can determine readily utilizable objects from images and serves to bridge the gap between GIS spatial analysis and image processing for modelling land objects based on spectral and spatial information simultaneously (Thouret et al., 2015; Simionato et al., 2021). OBIA can be applied to an object that consists of grouped pixels. It uses spectral and textural neighborhood relationships and shape characteristics information to classify objects (Amatya et al., 2021; Lima et al., 2021). Additionally, the rule-based approach allows users to apply local variation to analyses and that it can take advantage of user's knowledge at various stages of the classification approach (Najafi et al., 2021).

In the last decade, the application of OBIA for geomorphological landform detection and mapping has increased significantly (Drăguţ and Blaschke, 2006; Martha et al., 2010; Hölbling et al., 2012; Minar et al., 2018; Comert et al., 2019; Bandura et al., 2021), and detection of volcanic landforms (Van Asselen and Seijmonsbergen, 2006; Kassouk et al., 2014; Thouret et al., 2015; Feizizadeh et al., 2021a). Several researchers also have applied remote sensing datasets, including LiDAR, airborne laser scanning, and digital elevation model for karst landforms identification and mapping (Waele et al., 2015; Silva et al., 2017; Hofierka et al., 2018; Garcia and Grohmann, 2019; Su et al., 2021). In this regard, the present study represents a new semi-automated fuzzy object-based approach to detect and map a karst area and its landforms, including Dolin, Ouvala, Lapiez, Canyon, Polje and Karren. Therefore, we use Sentinel 2 images and auxiliary data such as a DEM and its derivatives (e.g. slope, flow direction, flow accumulation) in the case study areas of Takht-Soleiman and Parave-Biston mountains northwest and west Iran, respectively.

2. Location and geomorphological properties of the study areas and datasets

2.1. Case study area 1

Takht-Soleiman is situated in northwest Iran (Fig. 1) and is a tourist destination because of its historical monuments such as Azergoshnasb temple and Soleiman prison. From a geological perspective, the Takht-Soleiman basement rocks are Precambrian. The geological activities of the area have included repeated episodes of

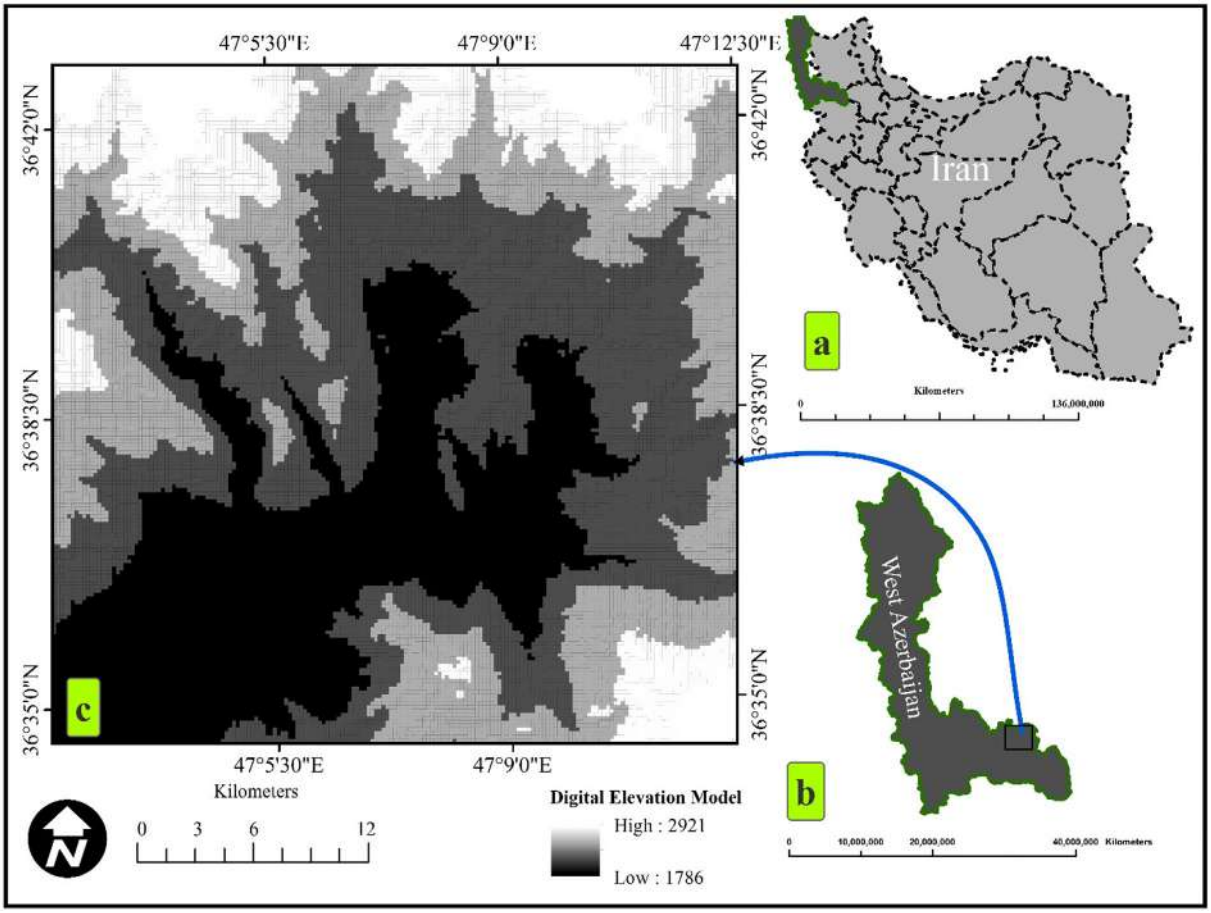

Fig. 1. Location of case study area 1, a) in Iran, b) in the west Azerbaijan province, and c) in Takht-Soleiman.

orogenous activity, rifting, sedimentation and magmatism (Rezaei Moghaddam et al., 2011). The formations of the Takht-Soleiman area include various rock types of metamorphic, igneous and sedimentary origin that span in age from the Precambrian to the Cenozoic (Geology organization of Iran, 2012). The sequence of rock formations in the area is as follows: Precambrian metamorphic rocks, Precambrian and Cambrian sedimentary rocks, Paleozoic metamorphic rocks, Oligocene sedimentary and volcanic rocks and Pliocene and young Quaternary deposits (Omrani et al., 2020). Most of the study area is covered by metamorphic rocks (Gneiss, Amphibolite, Mica and Schist). These types of rocks are characterized by rough topography that forms at the highest altitudes (Rezaei Moghaddam et al., 2011). Fig. 2 represents the geological features of Takht-Soleiman.

2.2. Case study area 2

The Parave-Biston Mountain (with an area of 879.3 k^2) is located in the northeast of Kermanshah province, in west Iran (Fig. 3). The Parave-Biston Mountain is a limestone mass dating back to the Triassic to late Cretaceous (Entezari and Aghaeipour, 2018). The evaluation of exo-karst formations in the Parave-Biston Mountain indicates that the dissolution process at various levels has created a particular landscape and topography (e.g., karst zones and landforms) with a specific geomorphic signature. It is characterized by underground drainage systems with sinkholes and caves (Billi et al., 2016). The wider area of Parave-Biston Mountain is covered by limestone that formed at the end of the Cretaceous on the folded Zagros mountain range. Therefore, the complex and utterly failed construction in this area reflects the intense orogenous activities in the past and present that have led to the development of various karst landforms. Fig. 4 represents the geological features of Parave-Biston as second case study area (Karimi and Sharafi, 2016).

2.3. Datasets

We used Sentinel 2 images with a spatial resolution of 10 m to detect and map the karst landforms. Topographic maps acquired in digital format from the Iranian National Cartographic Center were properly processed to generate Digital Elevation Models (DEMs) of each area. We then applied all reformatting and editing and produced the digital elevation model. Next, we employed spatial analysis in ArcGIS 10.4.1 to derive the secondary data, namely the slope, aspect, flow direction, curvature, hillshade, and flow accumulation to integrate the satellite images and GIS dataset for the detection and mapping of the karst landforms. In addition, the field observation dataset was collected by GPS in both case study areas. We collected 210 GPS control points (both point and polygon recorded by GPS) for both study areas to be used as training data and as ground control points to validate the results. Geological and geomorphological maps of the study areas were also considered for the validation analysis and accuracy assessment.

3. Methodology

OBIA comprises three main steps, namely segmentation, classification, and accuracy assessment (Kassouk et al, 2014). To detect

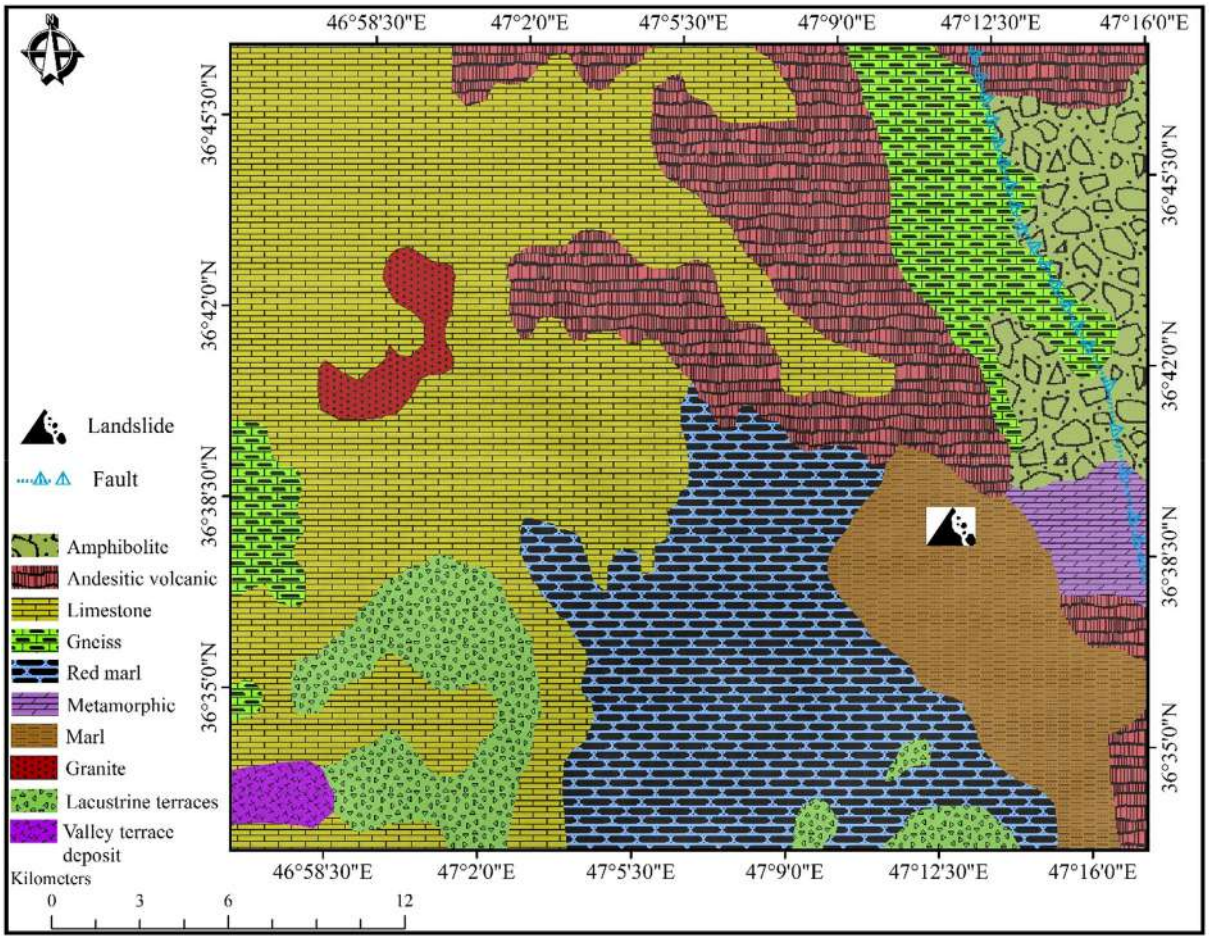

Fig. 2. Geological features of Takht-Soleiman as the first case study area (Geology organization of Iran, 2012).

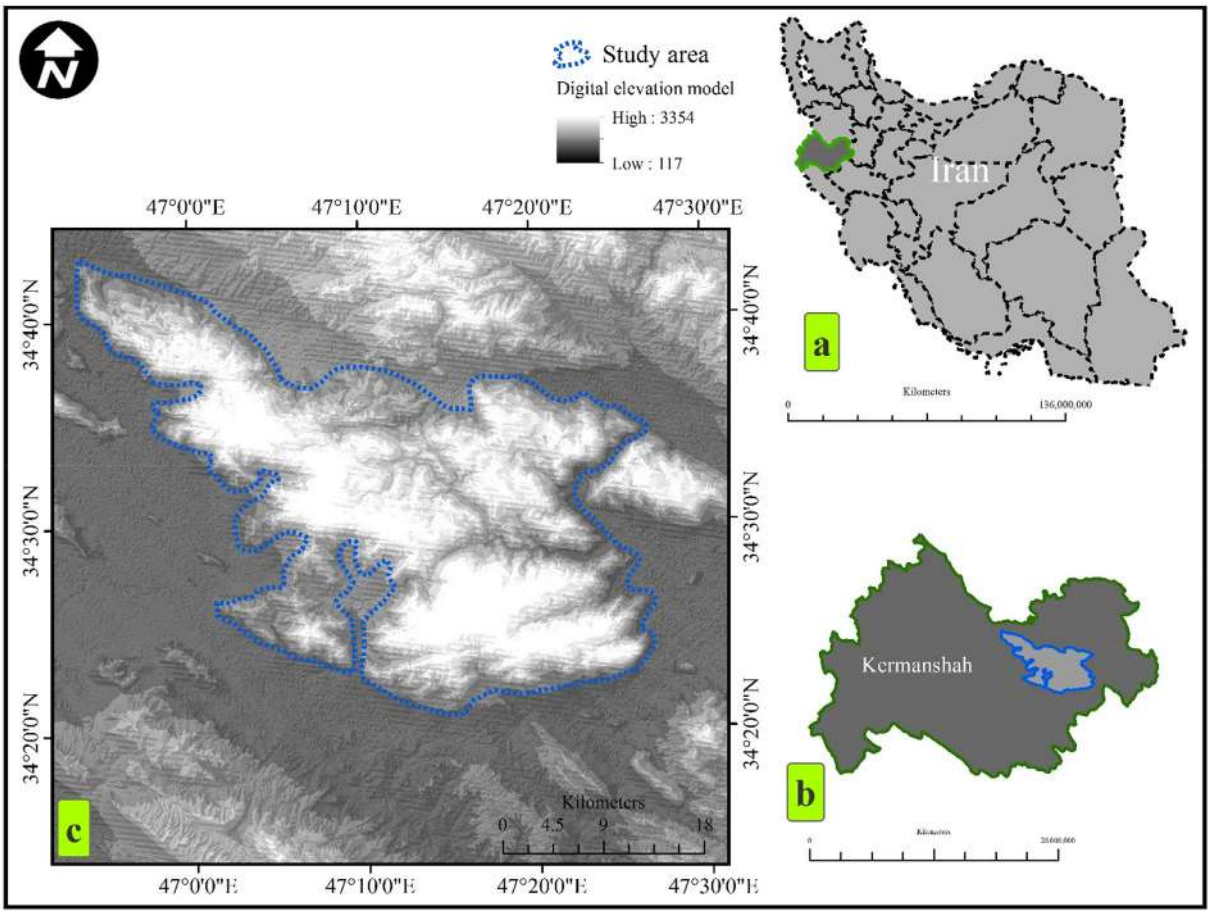

Fig. 3. Location of case study area 2, a) in Iran, b) in Kermanshah province, and c) in Parave-Biston.

and delineate karst areas and associated landforms, we first employed a multi-resolution segmentation algorithm on satellite images followed by a fuzzy rule-based classification in eCognition software from Trimble Geospatial. In the third stage, the FSE method is applied to determine the accuracy of the classification results (Fig. 5).

3.1. Image segmentation

Image segmentation is one of the most critical steps in object-based image analysis (Möller et al., 2007). The main aim of this process is to subdivide the digital image into smaller objects based on the spatial and spectral information (Feizizadeh et al., 2021b). Our present study emphasizes the applicability of the multi-resolution segmentation algorithm for generating the image objects for fuzzy rule-based classifications. The multi-resolution segmentation algorithm is a bottom-up region-merging segmentation algorithm that is frequently used for image segmentation in earth science (Liu et al., 2005; Blaschke, 2010). In multi-resolution segmentation, the scale factor is considered as the heterogeneity threshold for the color or spectral information. This factor also determines the proximity degree of the grey value to each other in an image object (Attarzadeh and Momeni, 2012). Determining an appropriate scale parameter, shape and compactness factors are critical in the segmention process to carry out a successful image analysis (Blaschke et al., 2014). Thus, several scale parameters were examined based on previous experience and using an iterative "trial-and-error" approach to achieve the most appropriate scale parameter, shape and compactness factors. Table 1 shows the segmentation parameters we used in this study to identify and detect the karst zones and landforms. Fig. 6 also depicts various segmentation scales employed to achieve an appropriate scale and its parameters.

3.2. Classification and selection of efficient object-based features

The classification is commonly based on rulesets in the OBIA methodology. The rulesets describe the relationships between properties and may have weighting factors. The object features have properties such as color, shape, texture, scale and area. Class-associated features include a connection to nearby objects and features such as statistical similarities and nearest neighbor (Amatya et al., 2021). To identify and detect the karst zones and landforms, we included the obtained fuzzy membership degrees of the sample objects as the experimental information. Each object was classified based on various features, including geometric characteristics and the average pixel information per object (Ruggeri et al., 2021; Kazemi Garajeh et al., 2022). To calculate the membership degree values of the functions, we tried to select a pure object from the karst zones and respective landforms separately to allocate a set of membership values (i.e. a number of values) for each selected function. We then employed a total of 22 appropriate object-based features (e.g. spectral, shape and textural features) to compute a fuzzy membership degree. We also applied the Approximate Gaussian function to obtain the fuzzy membership values of each feature. Table 2 indicates the object-based features used to calculate the fuzzy membership degree.

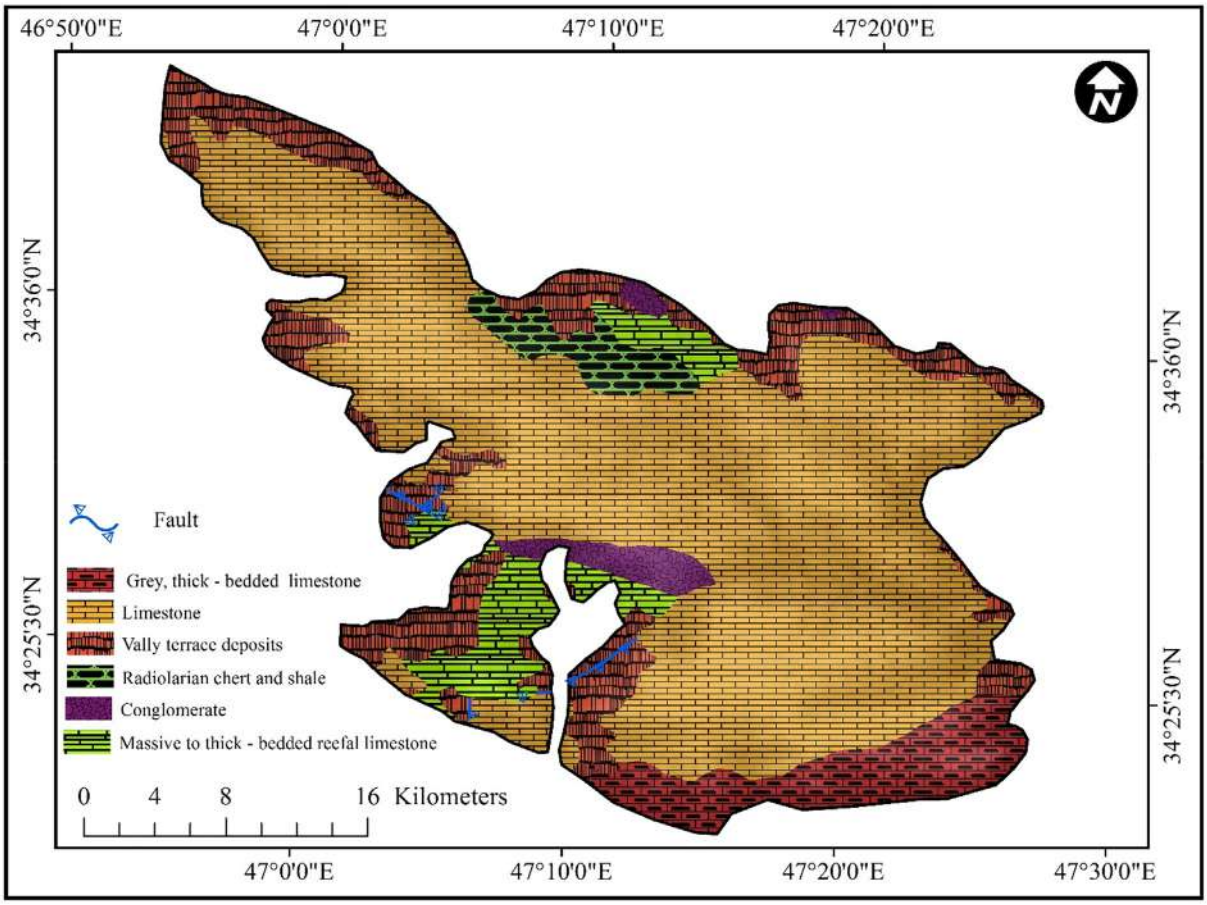

Fig. 4. Geological features of Parave-Biston as the second case study area (Geology organization of Iran, 2012).

3.3. Validation analysis

We used the Fuzzy Synthetic Evaluation (FSE) approach to obtain the accuracy of the classification results. The FSE is based on a sufficient combination of linguistic fuzzy operators (Sarmento et al., 2008). In this context, the main purpose of the FSE approach is to integrate the matches and non-matches that exist between a map classified using the fuzzy technique and a reference map (Pontius and Cheuk, 2006). The FSE allows us to estimate the overall and per-class accuracy of a classified map using the weighted sum of sample observation proportions in each *Difference* category per class in the map (Sarmento et al, 2008). The *Difference* categories were weighted based on the proportion of area occupied per primary and alternate reference landform classes in each sample observation. For instance, a maximum area of 91% is occupied by Canyon landform in VHCC situations (see Table 3 for further understanding).

We assume our classes as N in the classified map labelled as C_1 to C_N, organized as a set of labels $\Omega = \{C_1 to C_N\}$, and that a piece sample observation is allocated to only one class and only one *Difference* category $D = \{VHCC, \cdots, VHE\}$. If $P_{N,d}$ is the proportion of sample observations from map class C_N in Difference category d and W_d the respective weight defined for the FSE appliance, then, the computed accuracy P_N for map class C_N can be computed as per equation (3).

$$P_{N=\sum dP_{N,d}} \times W_d \tag{3}$$

To apply the FSE approach, we used field observation data collected by GPS in both case study areas as reference data and computed the respective confidence levels of FSE (Table 3).

4. Results

4.1. Detection and delineation of karst landforms

In this study, we developed an integrated OBIA and fuzzy rule-based classification approach and applied it to identify and map the karst zones and associated landforms, namely the Dolin, Ouvala, Lapiez, Canyon, Polje and Karren in the two study areas of Takht-Soleiman and Parava-Biston. Figs. 7–14 depict the observed and delineated karst landforms.

Table 4 gives the results of the accuracy assessment based on FSE for the study areas. As the results of the validation indicate, all of the considered landforms are outlined and delineated with an appropriate level of confidence (>95%).

5. Discussion

In this study, we applied a semi-automated OBIA approach to identify and map karst landforms. The result of the FSE approach indicates that the karst zones in the Takht-Soleiman and Parave-Biston mountain study areas and the associated classes of Dolin (96.8%), Ouvala (99.2%), Lapiez (95.1%), Canyon (98.3%), Polje (96.1%) and Karren (97.4%) landforms were validated with a satisfactory accuracy. The present study represents a significant step towards the development and implementation of a flexible, low cost and semi-automated fuzzy-OBIA approach for landform detection and delineation. Previous researchers (e.g., Waele et al., 2015; Silva et al., 2017; Hofierka et al., 2018; Garcia and Grohmann, 2019; Su et al., 2021) have employed remote sensing datasets for karst zone and associated landform detection and delineation. This

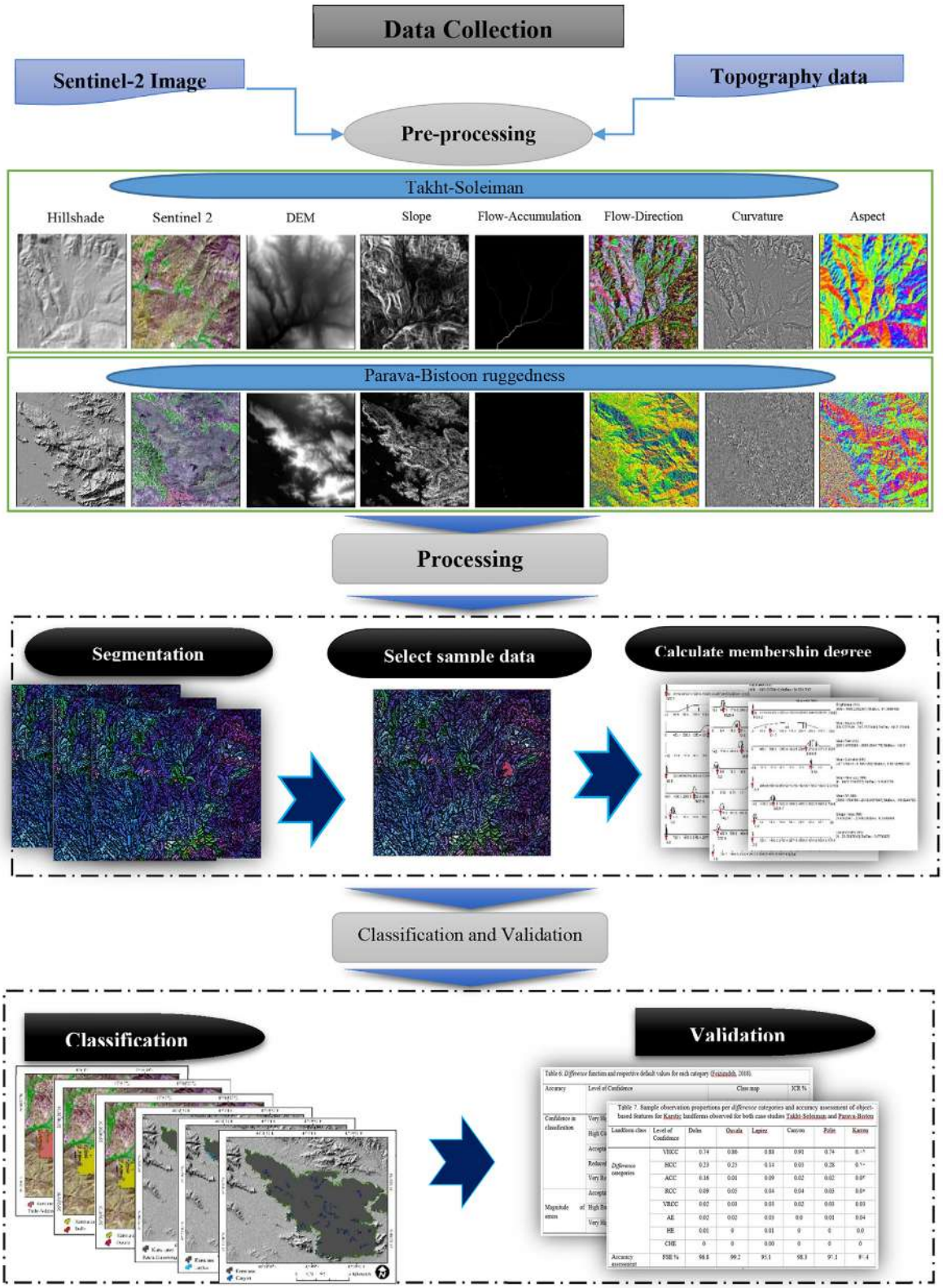

Fig. 5. The methodology of this study.

Table 1
The various segmentation parameters used for identifying the karst zones and landforms.

Karst area and their landforms	Segmentation algorithm used	Scale parameter	Shape factor	Compactness factor
Karst area of the Takht-Soleiman	Multi-resolution segmentation algorithm	600	0.6	0.4
Karst area of the Parava-Bistoon mountain		600	0.6	0.4
Dolin		550	0.8	0.2
Ouvala		570	0.8	0.2
Lapiez		350	0.4	0.6
Canyon		500	0.4	0.6
Polje		700	0.4	0.6
Karren		700	0.4	0.6

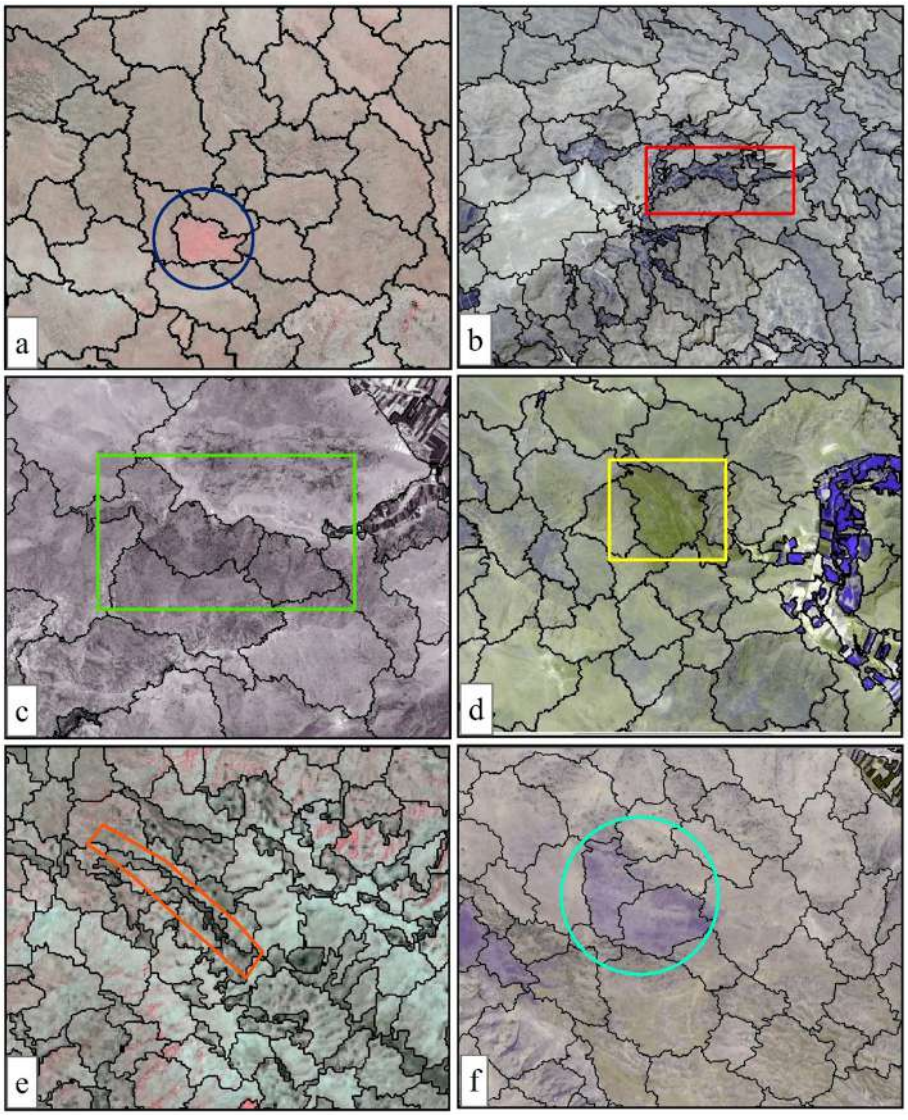

Fig. 6. The segmentation scales applied to Sentinel 2 image; a: 550 (Dolin), b: 350 (Lapiez), c: 700 (Karren), d: 700 (Polje), e: 500 (Canyon), f: 570 (Ouvala).

Table 2
Membership degrees obtained using the Approximate Gaussian function for features.

Faeture	Case study 1	Case study 2	Dolin	Ouvala	Lapiez	Canyon	Polje	Karren
Brightness	1	1	0	0	0	0	0	0
Mean hillshade	0	0	0.903	0.881	0	0	0	0
Mean elevation	0	0	0	0	0.901	0.891	0	0.901
Mean flow direction	0	0	0.993	1	0.952	0.972	0.912	0
Mean flow accumulation	0	0	0	0	0	0	0	0.991
Mean aspect	0	0	0	0	0.948	0	0	0.965
Mean slope	0	0	0	0	0.962	0.993	0	0
Mean band 2	0	0	0	0	0	0	0.903	0
STD band 3	0	0	0	0	0	0	0.92	0
STD flow direction	0	0	1	0.980	0	0	0.936	0
STD curvature	0	0	0	0	0.909	0	0	0
Length/width	0	0	0	0	0	0.963	0	0.932
Area	0	0	0.977	0.956	0	0	0	0
Border length	0	0	0.963	0	0	0	0	0
Asymmetry	0	0	0	0	0	0	0.945	0.914
Main direction	0	0	0	0	0	0	0	0.902
Shape index	0	0	0.942	0.965	0.969	0.975	0.958	0
Compactness	0	0	0	0	0.97	0	0	0
Roundness	0	0	0	0	0.930	0	0	0
Density	0	0	0	0	0.920	0	0.919	0
GLCM contrast	0.992	0.989	0	0	0	0	0	0
GLCM STD	0.985	0.982	0.972	0	0	0	0	0

Table 3
Difference function and respective default values for each category.

Accuracy	Level of Confidence	Class map		ICR %
		Demand class	Alternative class	
Confidence in classification	Very High Confidence in Classification (VHCC)	*		≥ 90
	High Confidence in Classification (HCC)	*		≥ 85
	Acceptable Confidence in Classification (ACC)		*	≥ 80
	Reduced Confidence in Classification (RCC)	*		$80 \leq$
	Very Reduced Confidence in Classification (VRCC)		*	50
Magnitude of errors	Acceptable Error (AE)			$50 \leq$
	High Error (HE)			≥ 85
	Very High Error (VHE)			≥ 90

work is the first to employ a fuzzy object-based approach to detect and classify the karst zone and associated landforms. Our introduced approach was uniquely suited to identify and map a complicated and dynamic karst zone and its landforms. The approach we outline here is particularly promising for landform detection and delineation in other parts of the world. Our introduced approach can be used as a fast and low-cost tool for researchers and geomorphologists to detect and delineate the earth's landforms.

Fuzzy classification can typically be employed in many different ways, such as applying fuzzy classifiers, neural network approaches or softening the output of hard classifications (e.g., with the maximum likelihood method) (Feizizadeh, 2018). Nevertheless, using a soft classification based on membership values is considered to be a major advantage of the fuzzy approach (Hofmann et al., 2011). Object class membership values in fuzzy OBIA represent the likelihood of the object belonging to each class based on the membership function selected by experts or derived from training data. Therefore, classification uncertainty can be represented by objects that have relatively high membership values to more than one class or do not have sufficiently high membership values to belong to any class (Blaschke, 2010).

According to the results of our study, the OBIA approach performs best for karst landform detection and mapping. In the context of object-based karst landform detection, OBIA enables us to apply object features, spatial relationships and expert knowledge during the segmentation, classification and validation stages. In terms of the karst landform mapping, certain geometric features such as shape index, length/width, density, and roundness are considered more efficient features. The geometric features are based on image objects obtained from the segmentation process. The geometric properties can be rotation variant because of their raster-based images. As shown in Table 4, the geometric features such as shape index, roundness, density and compactness perform well in the identification and detection of karst landforms because of the landforms' specific shapes such as a circle (Dolin) and linear shape (Canyon). In terms of the textural features for karst zone and landform mapping, the grey-level co-occurrence matrix (GLCM) based on contrast and standard deviation was identified as the most efficient feature for karst landform mapping. Therefore, the textural features' GLCM was applied to evaluate the feasibility of the image objects to be in the karst zone and landform classes based on an analysis of sub-objects that are helpful for evaluating highly textured data according to the GLCMs. According to our results, combining spectral features such as the brightness and mean of object images with information derived from GIS spatial analysis such as elevation and its derivatives including flow direction, flow accumulation, slope, curvature, hillshade and aspect can be efficiently applied for karst landform mapping. The spatial and geometric features, including length/width, shape index, roughness also yielded a high level of confidence for karst landform mapping. To sum up, the analysis of the result of the present research indicates

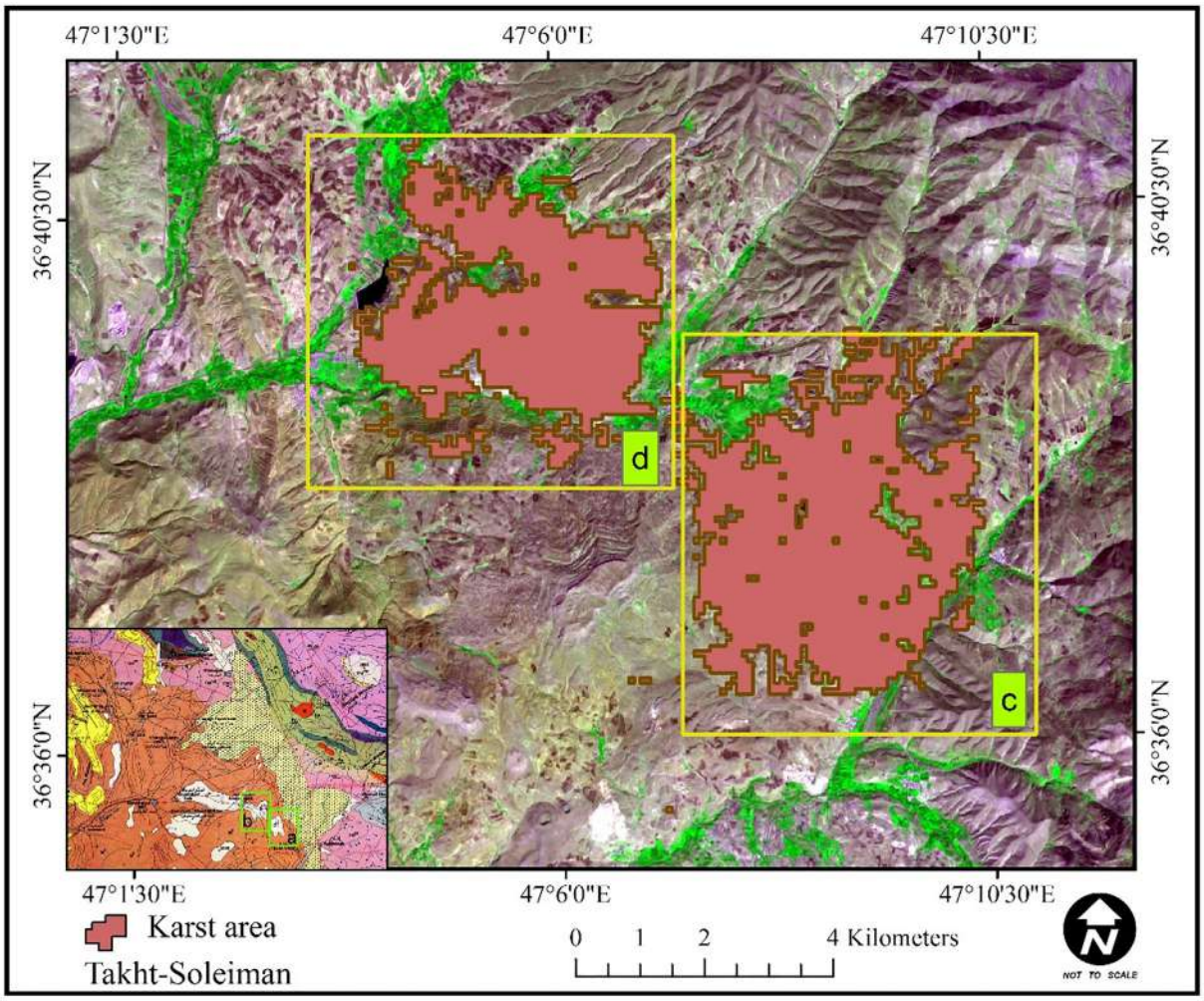

Fig. 7. Identified karst zones on, a, d) geological map, and c, d) identified kars zones on Sentinel-2 image using the Fuzzy-OBIA approach in Takht-Soleiman.

that the OBIA approach had optimal performance when comparing the segmented areas with the assessed ground truth for detecting and mapping the karst landforms.

In the use of fuzzy object-based remote sensing for the identification of karst zones and associated landforms, we have found one main challenge that refers fuzzy OBIA has not yet been widely applied for the detection and delineation of earth's dynamic landforms, thus creating difficulties in choosing an appropriate scale factor and function for various types of landform classification. Further research in this area should include the development of our approach to detect and map other karst landforms such as Tower, Glaciokarst, Cone and Fluvikarst. We also recommend future research regarding the efficiency of remote sensing-based spectral indexes such as Karst Bare-Rock Index (KBRI), Karst Rocky Desertification Synthesis Indices (KRDSI) and Spectral Mixture Analysis (SMA) for the precise detection and delineation of karst zones and associated landforms (Yue et al., 2009; Pei et al., 2018; Qi et al., 2019).

6. Conclusion and outlook

Review of the research literature indicates that previous studies identified and classified karst landforms primarily based on traditional techniques such as engineering geological classification, drilling and geophysical prospecting methods. In this paper, we present a new semi-automated object-based approach for detecting and mapping karst landforms. According to our results, the OBIA approach provides satisfactory results for detecting and mapping a karst area and its landforms. In the context of karst landform mapping, our study also provides detailed results regarding the efficiency of the use of object-based features instead of a per-pixel analysis. The results also reveal the unique capability of OBIA to integrate and combine data from various sources, which was indispensable for identifying and delineating some of the karst landforms. The good performance of our semi-automated approach for karst landform detection and mapping is based on the integration of OBIA and a fuzzy ruleset. The

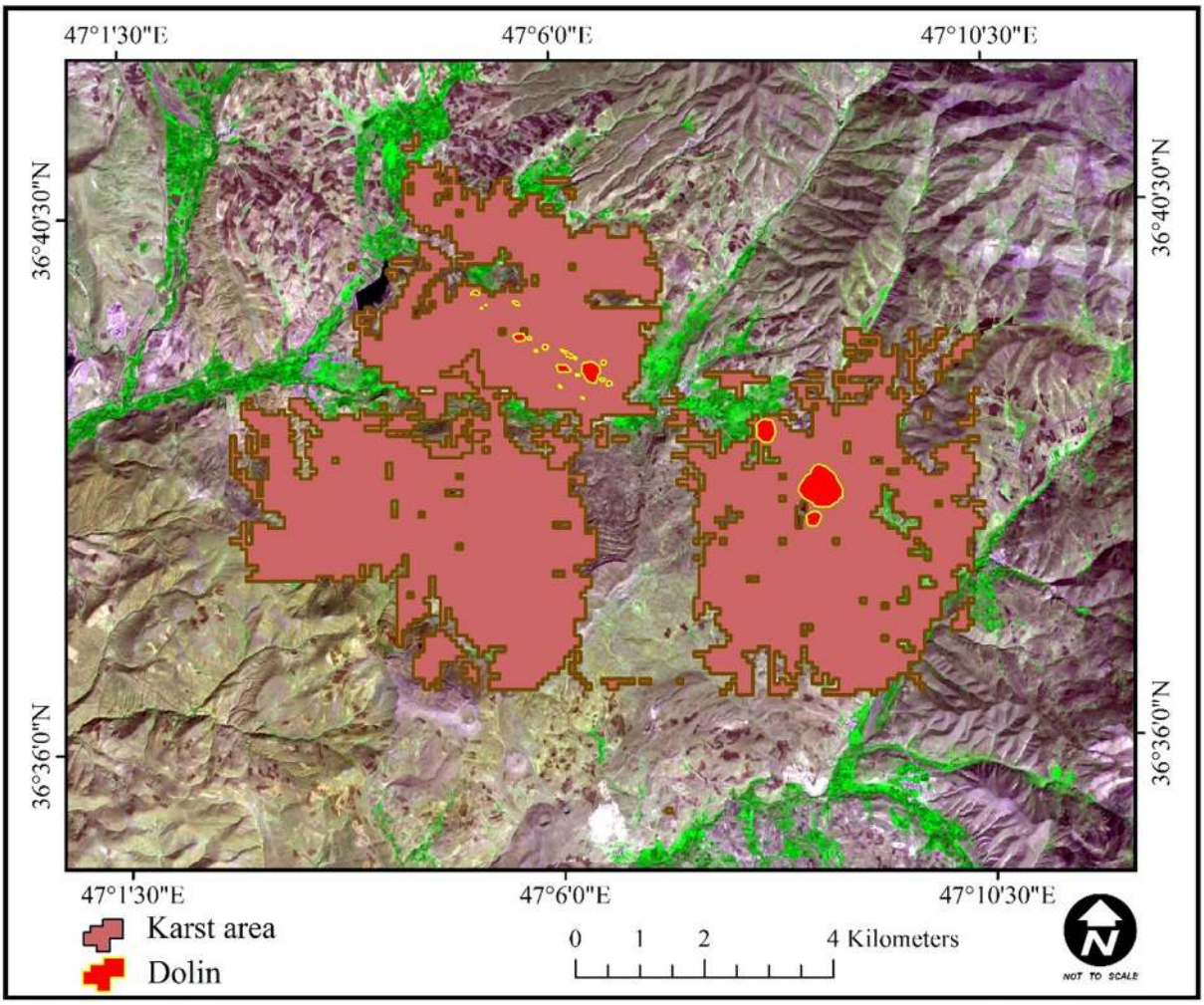

Fig. 8. Dolin landform detected using the Fuzzy-OBIA approach based on Sentinel-2 and auxiliary data in Takht-Soleiman.

outcome of this study can significantly contribute to developing the GIScience and OBIA frameworks. The nature of the semi-automated methodology allows us to transfer the developed ruleset and to apply it to karst landform mapping in other case studies after some adaptation and using different thresholds. The authors are confident that this will support future research in determining karst landforms cost-effectively and efficiently. Our results illustrate the high efficacy of the OBIA approach to improve the accuracy of existing geomorphological maps and for updating such maps.

Declaration of Competing Interest

The authors declare that they have no known competing financial interests or personal relationships that could have appeared to influence the work reported in this paper.

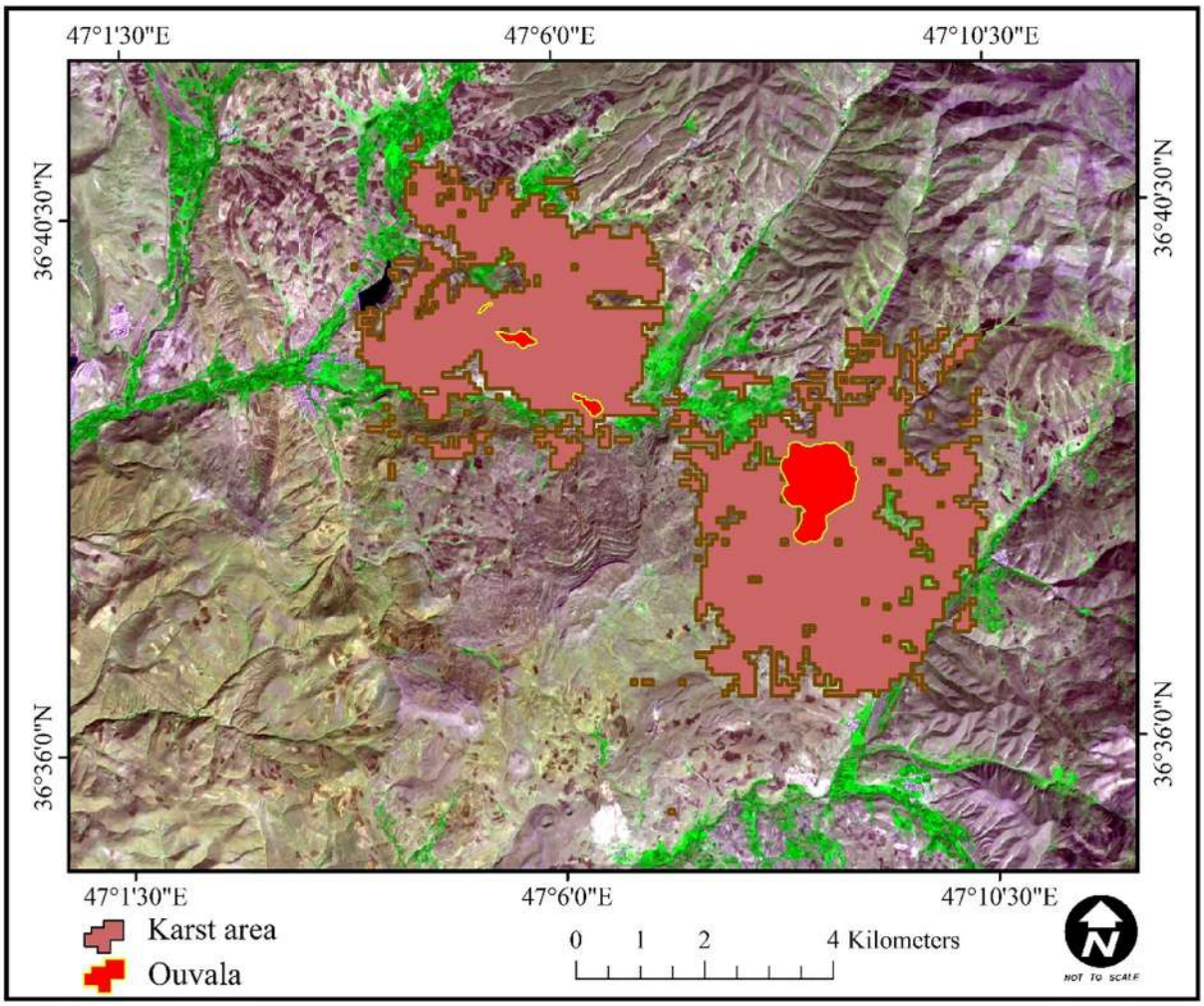

Fig. 9. Ouvala landform detected using the Fuzzy-OBIA approach based on Sentinel-2 and auxiliary data in Takht-Soleiman.

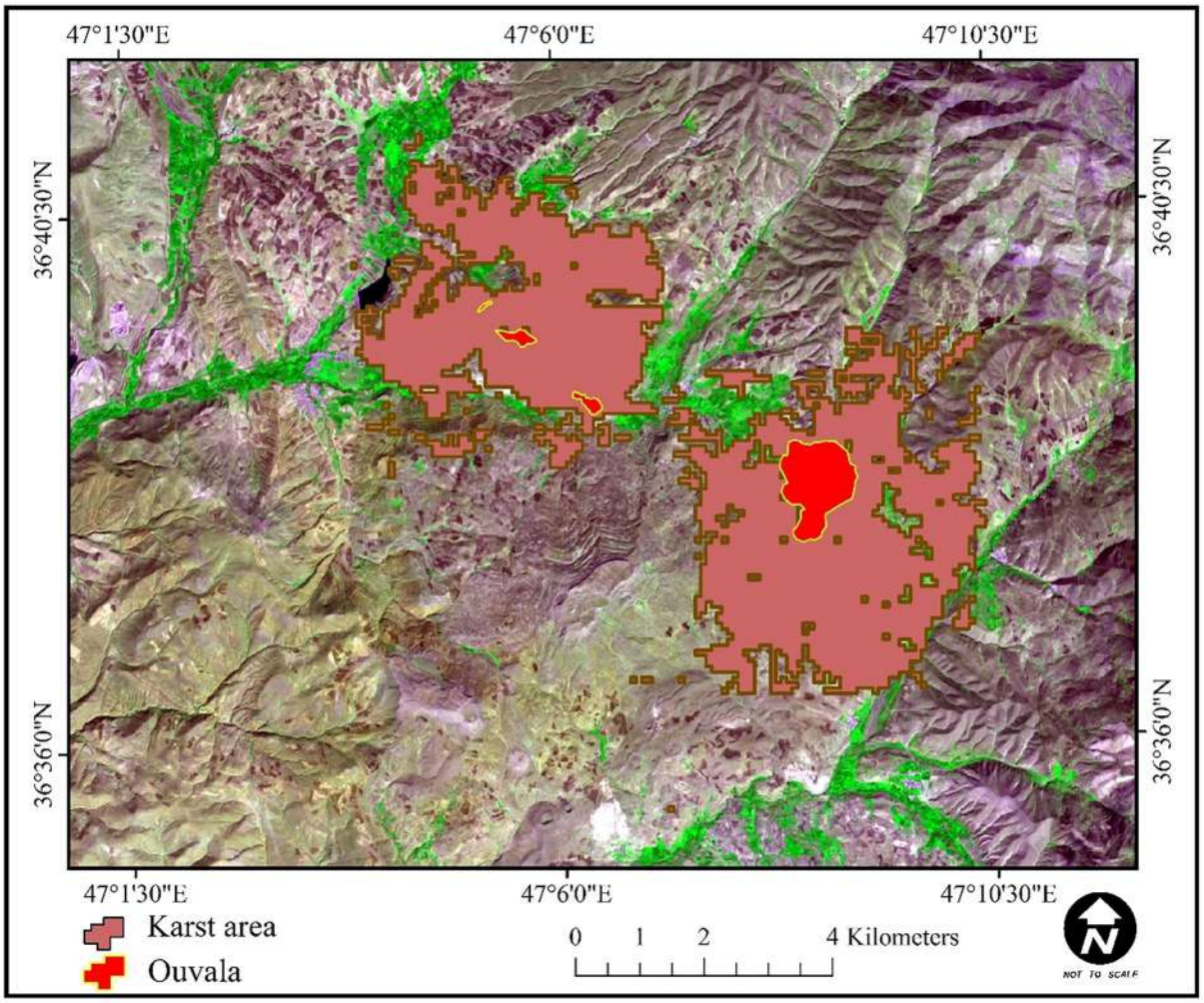

Fig. 10. Identified karst zone using the Fuzzy-OBIA approach in the Parava-Bistoon.

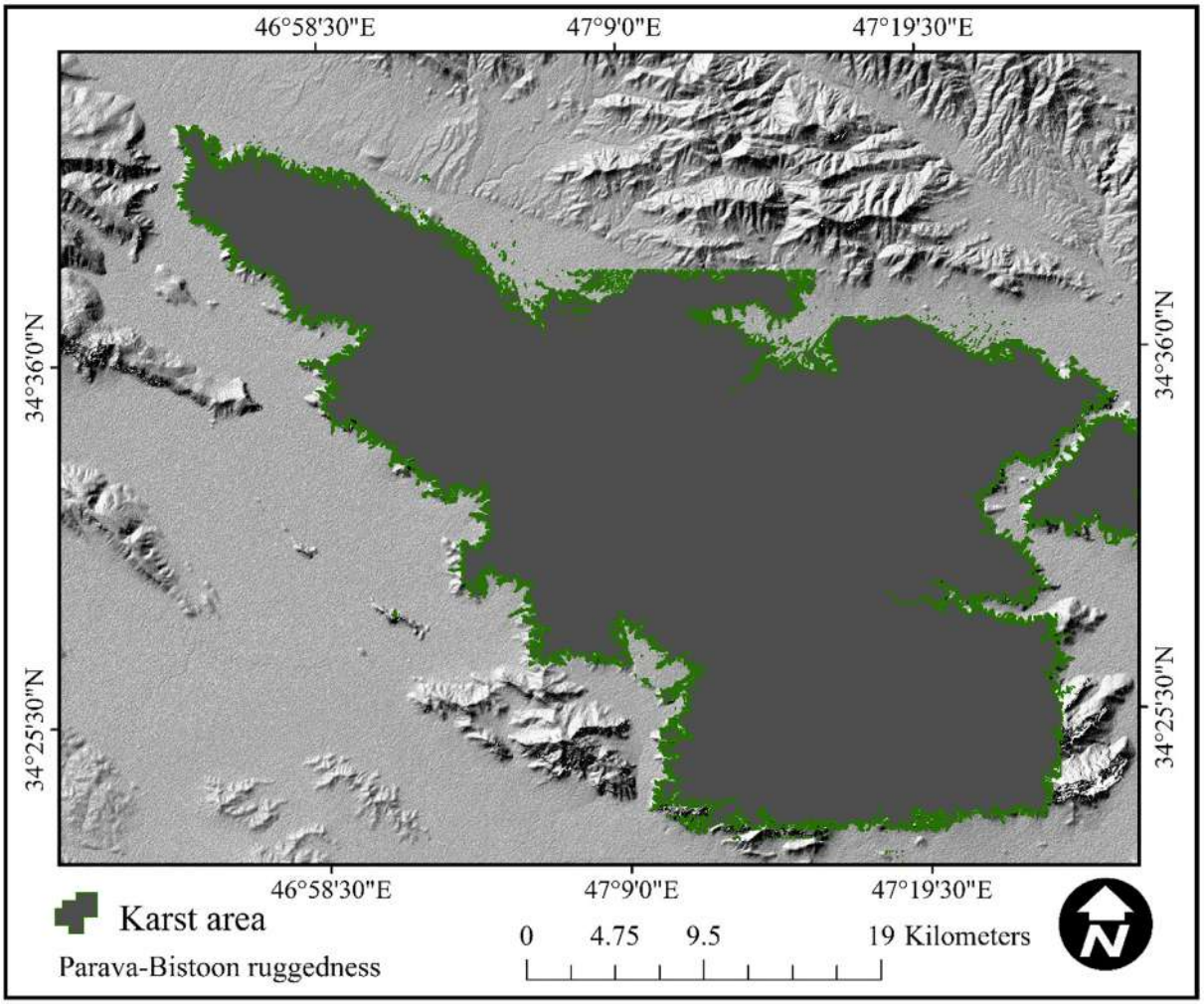

Fig. 11. Lapiez landform detected using the Fuzzy-OBIA approach in the Parava-Bistoon.

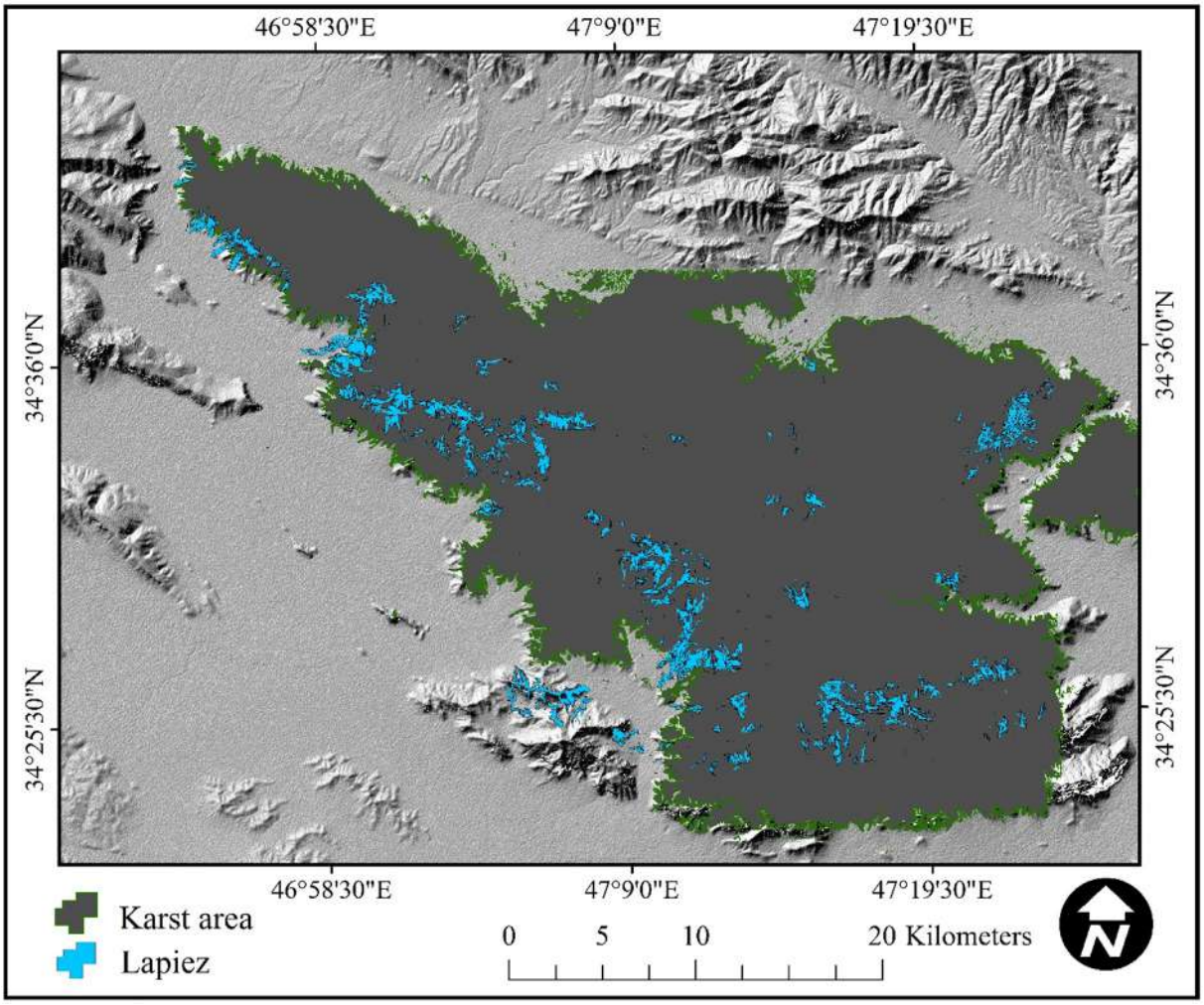

Fig. 12. Canyon landform detected using the Fuzzy-OBIA approach in the Parava-Bistoon.

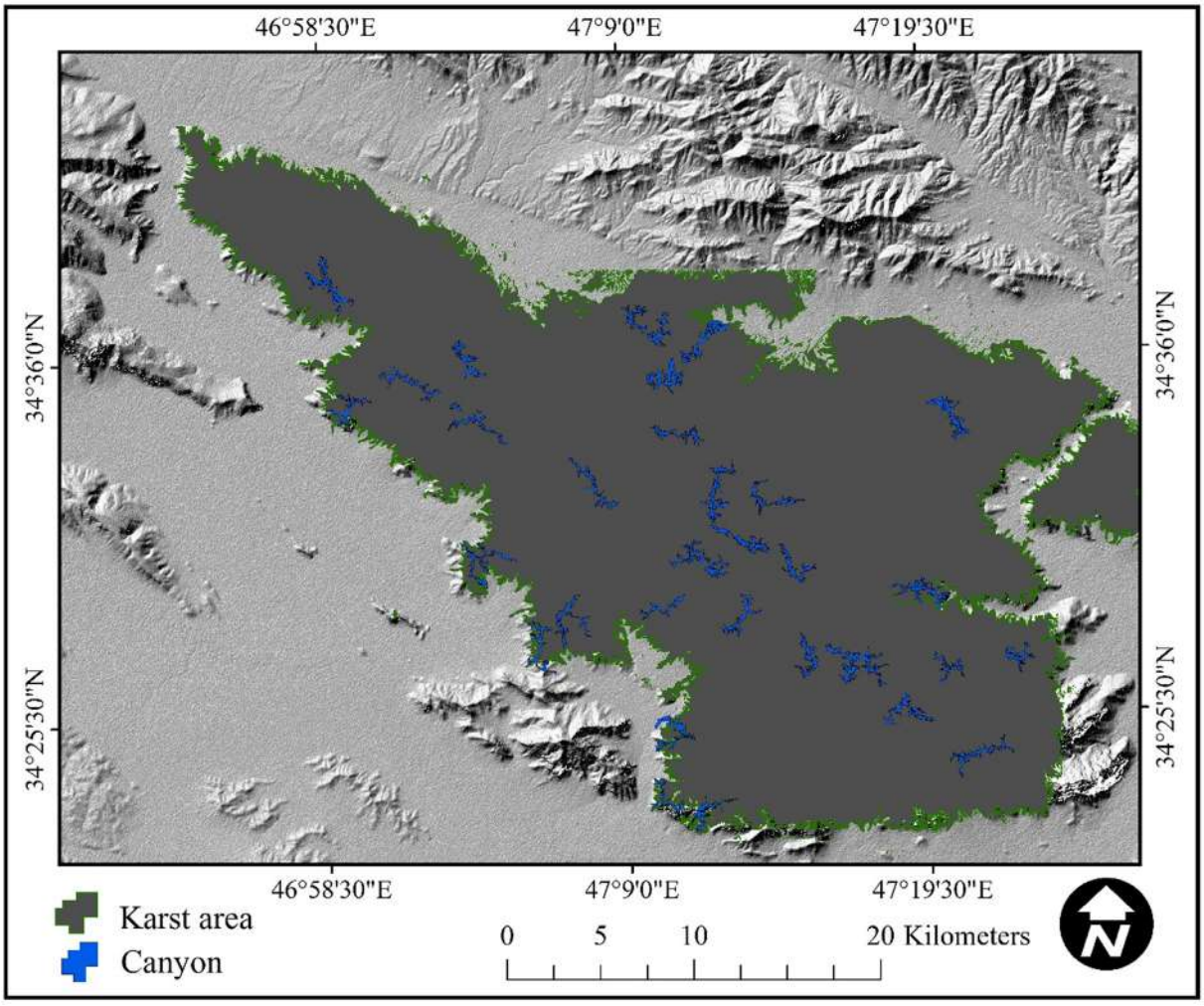

Fig. 13. Polje landform detected using the Fuzzy-OBIA approach in the Parava-Bistoon.

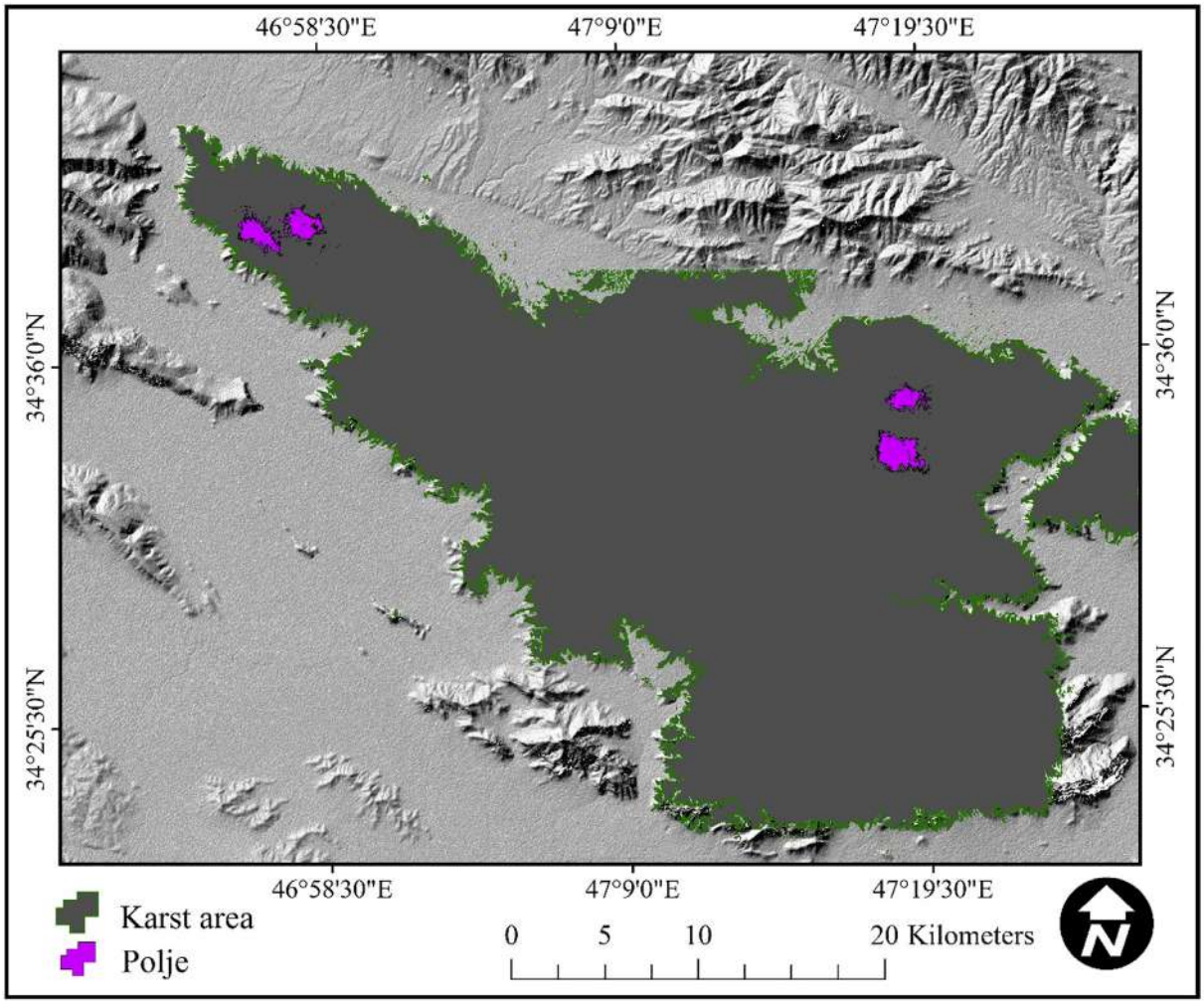

Fig. 14. Karren landform detected using the Fuzzy-OBIA approach in the Parava-Bistoon.

Table 4
Sample observation proportions per *difference* categories and accuracy assessment of object-based features for Karstic landforms observed for both case studies Takht-Soleiman and Parava-Biston.

Landform class	Level of Confidence	Dolin	Ouvala	Lapiez	Canyon	Polje	Karren
Difference categories	VHCC	0.74	0.86	0.88	0.91	0.74	0.81
	HCC	0.23	0.25	0.14	0.05	0.28	0.10
	ACC	0.16	0.01	0.09	0.02	0.02	0.03
	RCC	0.09	0.05	0.04	0.04	0.03	0.05
	VRCC	0.02	0.03	0.03	0.02	0.03	0.03
	AE	0.02	0.02	0.03	0.0	0.01	0.04
	HE	0.01	0	0.01	0	0	0.0
	CHE	0	0	0.00	0	0	0
Accuracy assessment	FSE %	96.8	99.2	95.1	98.3	96.1	97.4

References

Alexopoulos, J.D., Dilalos, S., Vassilakis, E., 2011. Adumbration of amvrakia's spring water pathways, based on detailed geophysical data (Kastraki - Meteora). Adv. Res. Aquatic Environ. 2, 105–112.

Amatya, P., Kirschbaum, D., Stanley, T., Tanyas, H., 2021. Landslide mapping using object-based image analysis and open source tools. Eng. Geol. 282.

Attarzadeh, R., Momeni, M., 2012. Object-Based Building Extraction from High Resolution Satellite Imagery. The International Archives of the Photogrammetry, Remote Sensing and Spatial Information Sciences. Melbourne, Australia.

Bandura, P., Minár, J., Bielik, M., 2021. Physically based morphostructural land surface segmentation: case of the Alps and Western Carpathians. Trans. GIS 25 (5), 2394–2418.

Billi, A., Filippis, L.D., Poncia, P.P., Sella, P., Faccenna, C., 2016. Hidden sinkholes and karst cavities in the travertine plateau of a highly-populated geothermal seismic territory (Tivoli, central Italy). Geomorphology 255, 63–80.

Blaschke, T., 2010. Object based image analysis for remote sensing. ISPRS J. Photogramm. Remote Sens. 65 (1), 2–16.

Blaschke, T., Feizizadeh, B., Hölbling, D., 2014. Object-based image analysis and digital terrain analysis for locating landslides in the Urmia Lake Basin, Iran. IEEE J. Selected Top. Appl. Erath Observ. Remote Sens. 7 (12), 4806–5481.

Chalikakis, K., Plagnes, V., Guerin, R., Valois, R., Bosch, F.P., 2011. Contribution of geophysical methods to karst-system exploration: an overview. Hydrol. J. 11, 1169–1180.

Comert, R., Avdan, U., Gorum, T., Nefeslioglu, H.A., 2019. Mapping of shallow landslides with object-based image analysis from unmanned aerial vehicle data. Eng. Geol. 260.

Drăguţ, L., Blaschke, T., 2006. Automated classification of land form elements using object-based image analysis. Geomorphology 81 (3-4), 330–344.
Drăguţ, L., Eisank, C., 2012. Automated object-based classification of topography from SRTM data. Geomorphology 141–142, 21–33.
Entezari, M., Aghaeipour, Y., 2018. Zonation of Surface Karst Development using Entropy Model (Case Study: Parâw - Bisetoon Mountain Masses). J. Geogr. Environ. Plann. 29, 8–21. In Persian.
Farooq, M., Park, S., Young, S., Kim, J.H., Mohammad, T., Adepelumi, A., 2012. Subsurface cavity detection in a karst environment using electrical resistivity (er): A case study from Yongweol-ri, South Korea. Earth Sci. Res. J. 16, 75–82.
Feizizadeh, B., 2018. A novel approach of fuzzy Dempster-Shafer theory for spatial uncertainty analysis and accuracy assessment of object-based image classification. IEEE Geosci. Remote Sens. Lett. 15, 18–22.
Feizizadeh, B., Blaschke, T., Tiede, D., Rezaei Moghaddam, M.H., 2017. Evaluating fuzzy operators of an object-based image analysis for detecting landslides and their changes. Geomorphology 293, 240–254.
Feizizadeh, B., Kazemi Garajeh, M., Blaschke, T., Lakes, T., 2021a. An object based image analysis applied for volcanic and glacial landforms mapping in Sahand Mountain, Iran. CATENA 198.
Feizizadeh, B., Garajeh, M.K., Lakes, T., Blaschke, T., 2021b. A deep learning convolutional neural network algorithm for detecting saline flow sources and mapping the environmental impacts of the Urmia Lake drought in Iran. CATENA. 207.
Garajeh, M.K., Feizizadeh, B., 2021. A comparative approach of data-driven split-window algorithms and MODIS products for land surface temperature retrieval. Appl. Geomatics 13 (4), 715–733.
Garajeh, M.K., Malakyar, F., Weng, Q., Feizizadeh, B., Blaschke, T., Lakes, T., 2021. An automated deep learning convolutional neural network algorithm applied for soil salinity distribution mapping in Lake Urmia, Iran. Sci. Total Environ. 778.
Garcia, G., Grohmann, C., 2019. DEM-based geomorphological mapping and landforms characterization of a tropical karst environment in southeastern Brazil. J. S. Am. Earth Sci. 93, 14–22.
Geology organization of Iran, 2012. www.gsi.ir.
Gerçek, D., 2010. Object-based classification of landforms based on their local geometry and geomorphometric context, Ph.D., Department of Geodetic and Geographic Information Technologies, Supervisor: Prof. Dr. Vedat Toprak Co-Supervisor: Prof. Dr. Josef Strobl March, 202 pages.
Groppelli, G., Viereck-Goette, L. (Eds.), 2010. Stratigraphy and Geology of Volcanic Areas. Geological Society of America Special, Colorado, United State, p. 291.
Hofierka, J., Gallay, M., Bandura, P., Šašak, J., 2018. Identification of karst sinkholes in a forested karst landscape using airborne laser scanning data and water flow analysis. Geomorphology 308, 265–277.
Hofmann, P., Blaschke, T., Strobl, J., 2011. Quantifying the robustness of fuzzy rule sets in object-based image analysis. Int. J. Remote Sens. 32 (22), 7359–7381.
Hölbling, D., Füreder, P., Antolini, F., Cigna, F., Casagli, N., Lang, S., 2012. A semi-automated object-based approach for landslide detection validated by persistent scatterer interferometry measures and landslide inventories. Remote Sens. 4, 1310–1336.
Kalhor, K., Ghasemizadeh, R., Rajic, L., Alshawabkeh, A., 2019. Assessment of groundwater quality and remediation in karst aquifers: a review. Groundwater Sustain. Dev. 8, 104–121.
Karimi, S., Sharafi, S., 2016. Comparative study of shape and slope changes using sinusoidal index in karst roughness of Kermanshah province. Geogr. Sci. (Appl. Geogr.) 12 (25), 50–69. In Persian.
Kassouk, Z., Thouret, J.C., Gupta, A., Solikhin, A., Liew, S.C., 2014. Object-based classification of a high-spatial resolution SPOT5 image for mapping geology and landforms of active volcanoes: Semeru case study, Indonesia. Geomorphology. 221, 18–33.
Kazemi Garajeh, M., Feizizadeh, B., Weng, Q., Rezaei Moghaddam, M.H., Kazemi Garajeh, A., 2022. Desert landform detection and mapping using a semi-automated object-based image analysis approach. J. Arid Environ. 199.
Lima, F., Blanco-Sepúlveda, R., Gómez-Moreno, M.L., Dorado, J., Peña, J.M., 2021. Mapping tillage direction and contour farming by object-based analysis of UAV images. Comput. Electron. Agric. 187.
Liu, Z., Wang, J., Liu, W.P., 2005. Building extraction from high resolution imagery based on multi-scale object oriented classification and probabilistic Hough transform. Int. Geosci. Remote Sens. Symposium (IGARSS) 4, 2250–2253.
Martha, T.R., Kerle, N., Jetten, V., Van Westen, C.J., Kumar, K.V., 2010. Characterizing spectral, spatial, and morphometric properties of landslides for semiautomatic detection using object-oriented methods. Geomorphology 116, 24–36.
Minar, J., Bandura, P., Holec, J., Popov, A., Drăguţ, L., Gallay, M., Hofierka, J., Kaňuk, J., Evans, I.S., 2018. Physically-based land surface segmentation: theoretical background and outline of interpretations. Geomorphometry 6, 270751.
Mohamed, I.N., Verstraeten, G., 2012. Analyzing dune dynamics at the dune field scale based on multi-temporal analysis of Landsat TM images. Remote Sens. Environ. 119, 105–117.
Möller, M., Lymburner, L., Volk, M., 2007. The comparison index: a tool for assessing the accuracy of image segmentation. Int. J. Appl. Earth Obs. Geoinf. 9 (3), 311–321.
Najafi, P., Navid, H., Feizizadeh, B., Eskandari, I., Blaschke, T., 2019. Fuzzy object-based image analysis methods using sentinel-2A and landsat-8 data to map and characterize soil surface residue. Remote Sens. 11 (21), 2583.
Najafi, P., Feizizadeh, B., Navid, H., 2021. A comparative approach of fuzzy object based image analysis and machine learning techniques which are applied to crop residue cover mapping by using sentinel-2 satellite and UAV imagery. Remote Sens. 13, 937.
Omrani, H., Fahimi, P., Mahmoodi, A., 2020. A data envelopment analysis game theory approach for constructing composite indicator: an application to find out development degree of cities in West Azarbaijan province of Iran. Socio-Econ. Plann. Sci. 69.
Pederson, G.B.M., 2016. Semi-automatic classification of glaciovolcanic landforms: an object-based mapping approach based on geomorphometry. J. Volcanol. Geoth. Res. 311, 29–40.
Pei, J., Wang, L., Huang, N., Geng, J., Cao, J., Niu, Z., 2018. Analysis of Landsat-8 OLI imagery for estimating exposed bedrock fractions in typical karst regions of Southwest China using a karst bare-rock index. Remote Sens. 10, 1321.
Pontius, R.G., Cheuk, M.L., 2006. A generalized cross-tabulation matrix to compare soft-classified maps at multiple resolutions. Int. J. Geogr. Inf. Sci. 20 (1), 1–30.
Putiska, R., Kusnirak, D., Dostal, I., Lacny, A., Mojzes, A., Hok, J., Pasteka, R., Krajnak, M., Bosansky, M., 2014. Integrated Geophysical and Geological Investigations of Karst Structures in Komberek, Slovakia. J. Cave Karst Stud. Natl. Speleol. Soc. Bull. 76 (3), 155–163.
Qi, X., Zhang, C., Wang, K., 2019. Comparing remote sensing methods for monitoring karst rocky desertification at sub-pixel scales in a highly heterogeneous karst region. Sci. Rep. 9, 13368.
Rezaei Moghaddam, M.H., Qadri, M.H., Moayed, M., 2011. Investigation of Dolins in Takht-e-Soliman region by cluster analysis method. Plann. Arranging Space 14, 191–214. In Persian.
Robson, B.A., Bolch, T., MacDonell, S., Hölbling, D., Rastner, P., Schaffer, N., 2020. Automated detection of rock glaciers using deep learning and object-based image analysis. Remote Sens. Environ. 250.
Ruggeri, S., Henao-Cespedes, V., Garcés-Gómez, Y.A., Parra Uzcátegui, A., 2021. Optimized unsupervised CORINE Land Cover mapping using linear spectral mixture analysis and object-based image analysis. Egypt. J. Remote Sens. Space Sci. 24 (3), 1061–1069.
Sarmento, P., Carrao, H., Caetano, M., 2008. A fuzzy synthetic evaluation approach for land cover cartography accuracy assessment. In: The 8th International Symposium on Spatial Accuracy Assessment in Natural Resources and Environmental Sciences, Shanghai China, pp. 348–355.
Silva, O., Bezerra, F., Maia, R., Cazarin, C., 2017. Karst landforms revealed at various scales using LiDAR and UAV in semi-arid Brazil: consideration on karstification processes and methodological constraints. Geomorphology 295, 611–630.
Simionato, J., Bertani, G., Osako, L.S., 2021. Identification of artisanal mining sites in the Amazon Rainforest using Geographic Object-Based Image Analysis (GEOBIA) and Data Mining techniques. Remote Sens. Appl.: Soc. Environ. 24.
Su, M., Liu, Y., Xue, Y., Cheng, K., Ning, Z., Li, G., Zhang, K., 2021. Detection method of karst features around tunnel construction by multi-resistivity data-fusion pseudo-3D-imaging based on the PCA approach. Eng. Geol. 288.
Thouret, J.C., Kassouk, Z., Gupta, A., Liew, S.C., Solikhin, A., 2015. Tracing the evolution of 2010 Merapi volcanic deposits (Indonesia) based on object-based classification and analysis of multi-temporal, very high resolution images. Remote Sens. Environ. 170, 350–371.
van Asselen, S., Seijmonsbergen, A.C., 2006. Expert-driven semi-automated geomorphological mapping for a mountainous area using a laser DTM. Geomorphology 78 (3-4), 309–320.
Vargemezis, G., Tsourlos, P., Stampolidis, A., Fikos, I., Ballas, D., Papadopoulos, N., 2012. A focusing approach to ground water detection by means of electrical and EM methods the case of Paliouri, Northern Greece. Studia Geophysica et Geodaetica. 56 (4), 1063–1078.
Waele, J.D., Gutierrez, F., Audra, P., 2015. Karst geomorphology: from hydrological functioning to palaeoenvironmental reconstructions. Part II. Geomorphology. 247, 1.
Waltham, A.C., Fookes, P.G., 2005. Engineering classification of karst ground conditions. Speleogenesis Evol. Karst Aqufers. 3, 1–20.
Yue, Y., Wang, K., Li, J., Zhang, B., Liu, B., Jiao, Q., Zhang, X., 2009. Developing new spectral indices for karst rocky desertification monitoring in Southwest China. IEEE Int. Geosci. Remote Sens. Symposium. IV-318-IV-321.
Zaidi, F.K., Kassem, O.M.K., 2012. Use of electrical resistivity tomography in delineating zones of groundwater potential in arid regions: a case study from Diriyah region of Saudi Arabia. Arab. J. Geosci. 5, 327–333.